united nations
educational, scientific
and cultural
organization

international atomic
energy agency

the
abdus salam
international centre for theoretical physics

SMR/1238-32

ADRIATICO RESEARCH CONFERENCE on

LASERS IN SURFACE SCIENCE

11-15 September 2000

Miramare - Trieste, Italy

Growth and surface reaction kinetics in thin film epitaxy studied by oblique-incidence reflectivity difference

X. D. Zhu
University of California at Davis
Davis - CA, United States of America

Growth and surface reaction kinetics in thin film epitaxy studied by *oblique-incidence reflectivity difference*

X.D. Zhu
University of California at Davis

- **Oblique-incidence reflectivity difference**

- **Growth kinetics in rare gas epitaxy on metals**
  Xe on Ni(111): commensurate substrate
  Xe on Nb(110): incommensurate substrate

- **Thermal annealing of ion-sputtered surfaces**
  Ne^+ sputtering and thermal annealing of Ni(111)

- **Surface oxidation kinetics in oxide epitaxy**
  $SrTiO_3$ and $La_{0.67}Ba_{0.33}MnO_{3-\delta}$ on $SrTiO_3(001)$

(Ariatico Research Conference on Lasers in Surface Science, 2000)

Oblique-incidence reflectivity difference technique

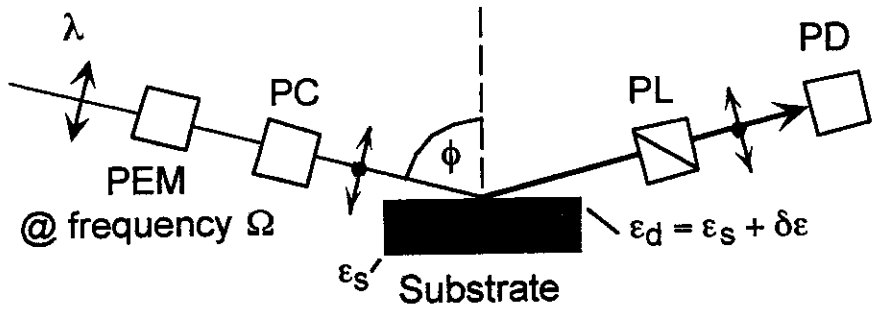

$$\Delta_s \equiv \left(r_s - r_{s0}\right)/r_{s0}$$

$$\Delta_p \equiv \left(r_p - r_{p0}\right)/r_{p0}$$

$$r_p = |r_p| e^{i\Phi_p} \cong |r_{p0}| e^{i\Phi_{p0}} \left(1 + \mathrm{Re}\Delta_p\right) e^{i\,\mathrm{Im}\Delta_p}$$

$$r_s = |r_s| e^{i\Phi_s} \cong |r_{s0}| e^{i\Phi_{s0}} \left(1 + \mathrm{Re}\Delta_s\right) e^{i\,\mathrm{Im}\Delta_s}$$

$$\Delta_p - \Delta_s \approx i\left\{\frac{4\pi(\cos\phi)(\sin\phi)^2 \varepsilon_s}{\lambda\left[\varepsilon_s^2(\cos\phi)^2 - \varepsilon_s + (\sin\phi)^2\right]}\right\}\int_0^d \frac{(\varepsilon_d - \varepsilon_s)(\varepsilon_d - 1)}{\varepsilon_d} dz$$

Reflected light intensity at 2Ω: (setting $|r_{p0}\cos\theta_{PL}| = |r_{s0}\sin\theta_{PL}|$)

$$I_{2\Omega} \cong I_{inc}|r_{p0}\cos\theta_{PL}|^2 \,\mathrm{Re}\{\Delta_p - \Delta_s\} \sim \mathrm{Re}\{\Delta_p - \Delta_s\}$$

Reflected light intensity at Ω: (setting $\phi_{PC} + (\phi_{p0} - \phi_{s0}) = 0$)

$$I_\Omega \cong I_{inc}|r_{p0}\cos\theta_{PL}|^2 \,\mathrm{Im}\{\Delta_p - \Delta_s\} \sim \mathrm{Im}\{\Delta_p - \Delta_s\}$$

Growth kinetics in rare gas epitaxy on metals

Layer growth (Frank-van der Merwe mode):

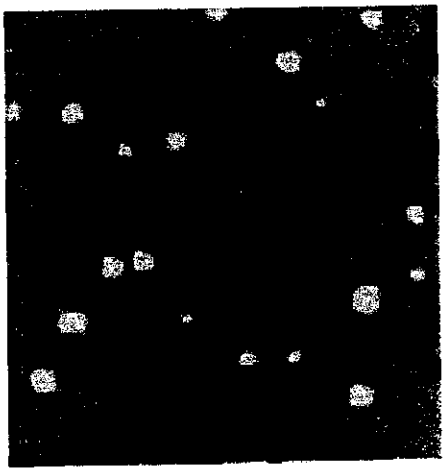

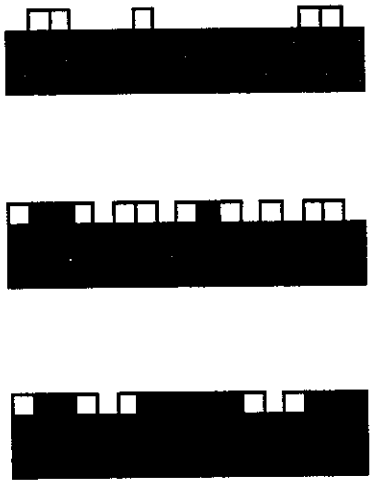

ε_d changes periodically.

Island growth (Volmer-Weber mode):

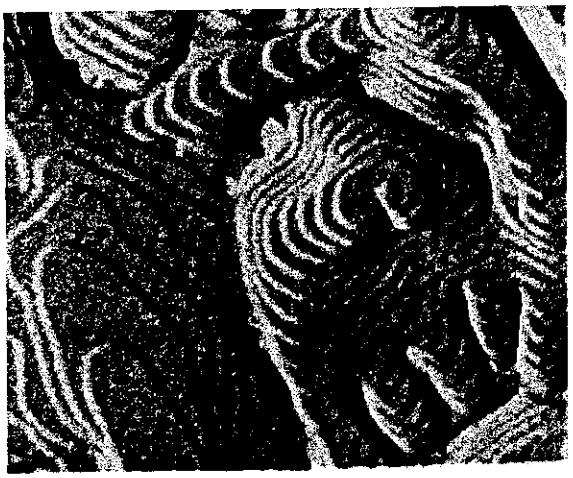

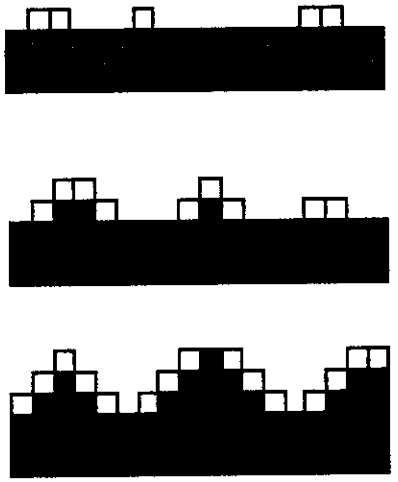

ε_d changes monotonically.

Step-flow growth:

ε_d remains constant.

Rare gas growth on commensurate substrate

Xe/Xe(111)/Ni(111)

LEED pattern of a commensurate $\left(\sqrt{3}\times\sqrt{3}\right)R30^\circ$ structure

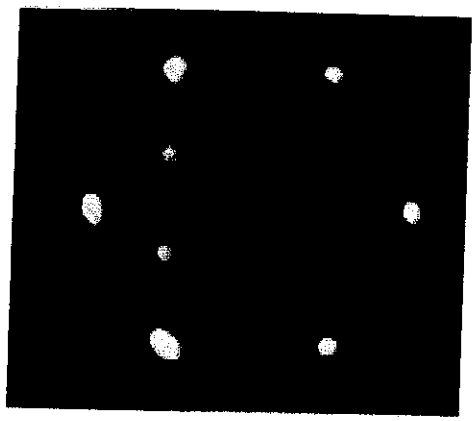

Real-space structure of a commensurate $\left(\sqrt{3}\times\sqrt{3}\right)R30^\circ$ structure

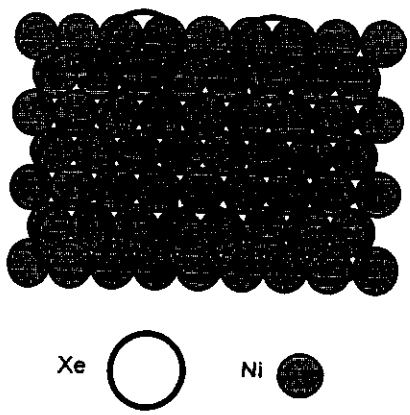

Growth of Xe multilayers on Xe(111)/Ni(111):

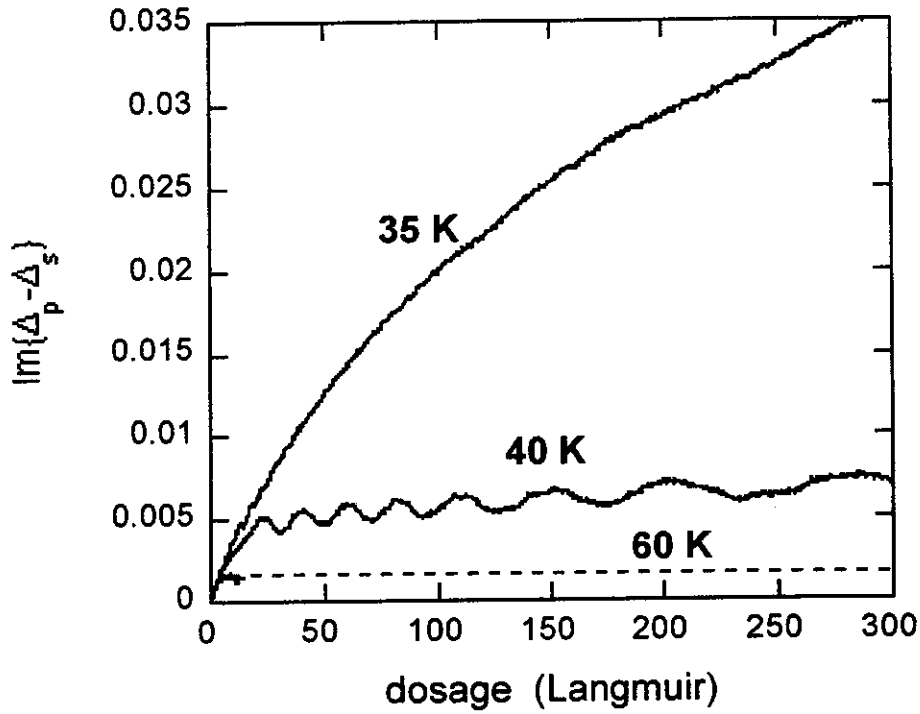

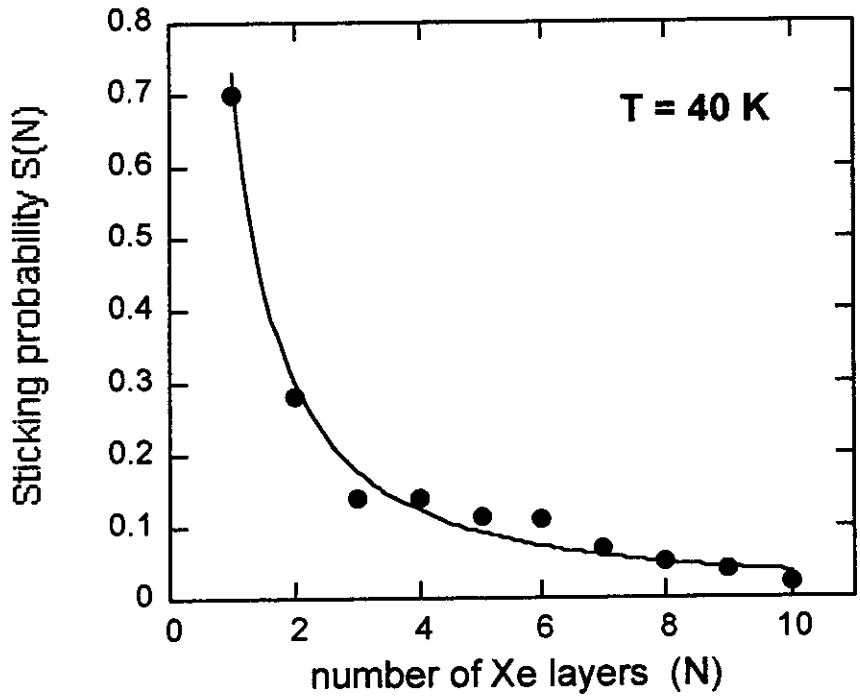

Transition from multilayer growth to layer-by-layer growth:

- Rate theory of nucleation and growth and kinetic Monte Carlo (KMC) simulation

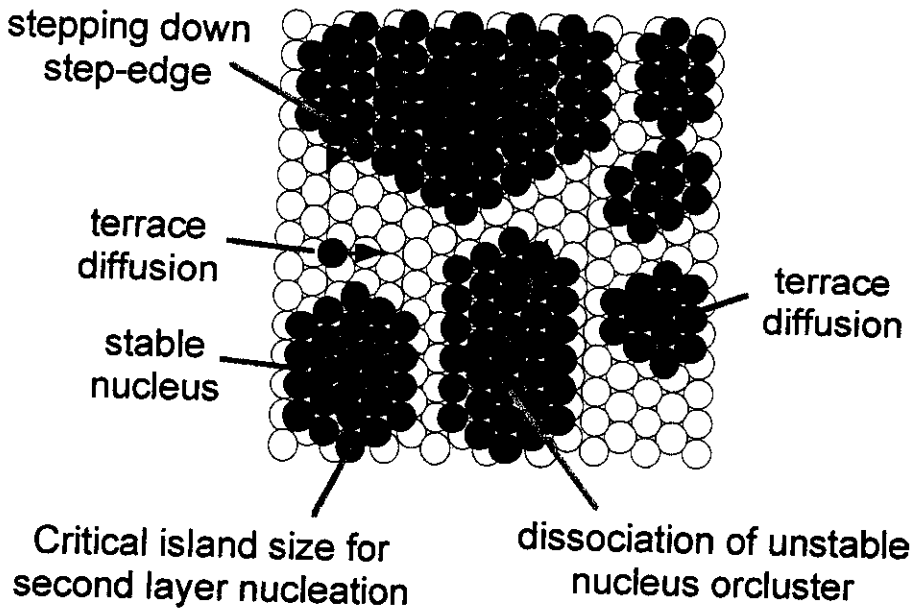

Stepping down a step edge: $h' = \nu_{SE} \exp\left[-\left(E_{SE} + E_d\right)/k_B T\right]$

Terrace diffusion: $h = \nu_d \exp\left(-E_d/k_B T\right)$

Critical size **i** for stable nuclei: 2-D nuclei with **i+1** atoms stable during deposition

Critical island size $\mathbf{R_c}$ for second layer nucleation: Probability of forming a stable nucleus on 2-D islands of radius $\mathbf{R_c}$ is 50%.

Nucleation theory and KMC: Transition in **i** and $\mathbf{R_c}$

Binding energies of Xe on Xe(111):

Xe binding energy across a Xe island

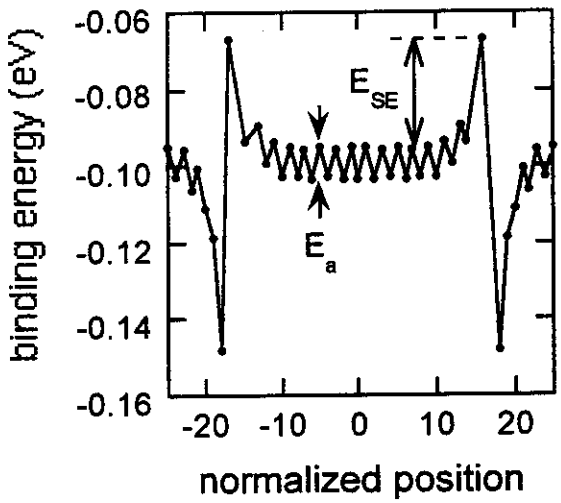

Terrace diffusion barrier: E_d = 8 meV
Extra step edge barrier: E_{SE} = 28 meV (Schwoebel-Ehrlich)

Binding energies of Xe 2-D clusters on Xe(111):

Single Xe-Xe bond: E_1 = 20 meV
Double Xe-Xe bond: E_2 = 40 meV
Triple Xe-Xe bind: E_3 = 60 meV

Kinetics Monte Carlo simulation and nucleation theory:

(1) For 23 K ≤ T ≤ 40 K, only Xe septamers or larger compact islands (**i ≥ 6**) are stable on Xe(111) against dissociation.

(2) From 35 to 40K, average island size $\mathbf{R_{av}}$ before coalescence remains unchanged.

(3) Critical radius $\mathbf{R_c}$ increases by one order of magnitude from 35 to 40 K, causes the transition from multilayer growth at 35 K to layer-by-layer growth at 40 K.

Thickness dependence of Xe sticking probability:

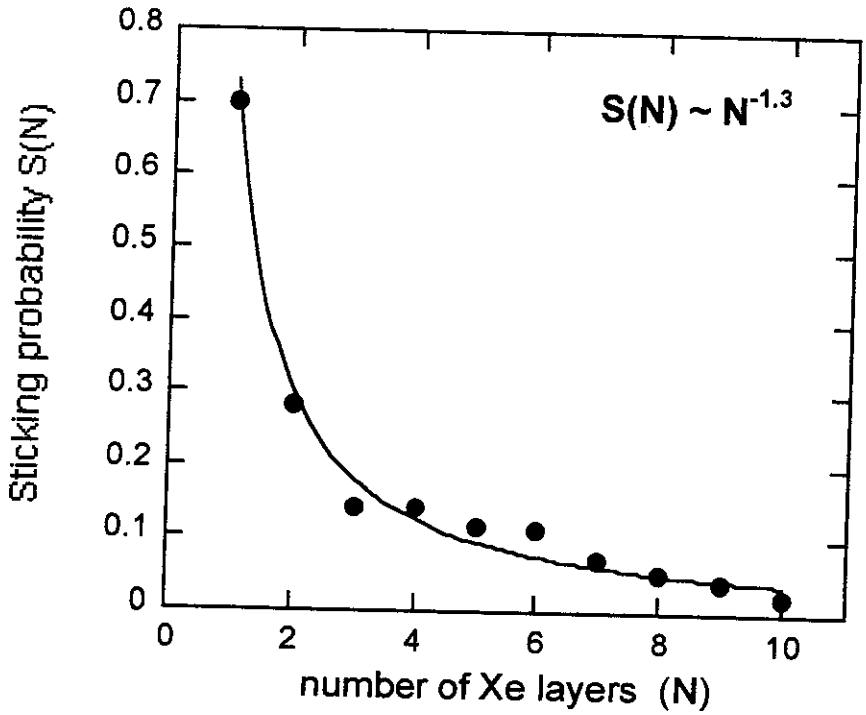

(1) Heavier Xe (M_{Xe}/M_{Ni} = 2.4) pushes lighter Ni surface atoms forward without being bounced kinematically and thus the interaction time is longer;

(2) Xe binding energy is larger near metallic Ni(111) due to additional polarization effects; it is the largest on Ni(111) due to charge transfer.

Both favor larger sticking probability on thinner Xe films.

Growth of Xe multilayers on incommensurate Nb(110)

0.1°-miscut, $L_t \approx 1300$Å

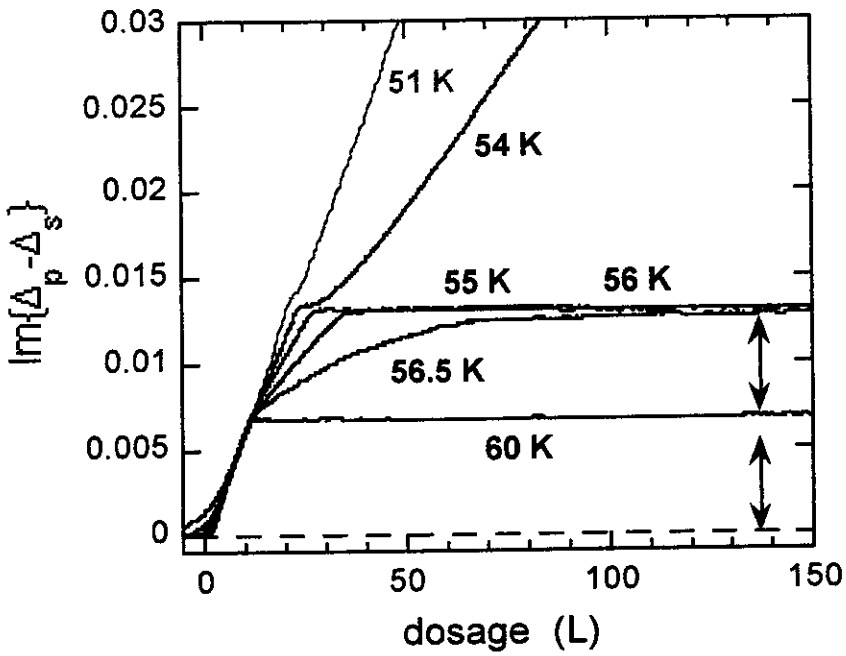

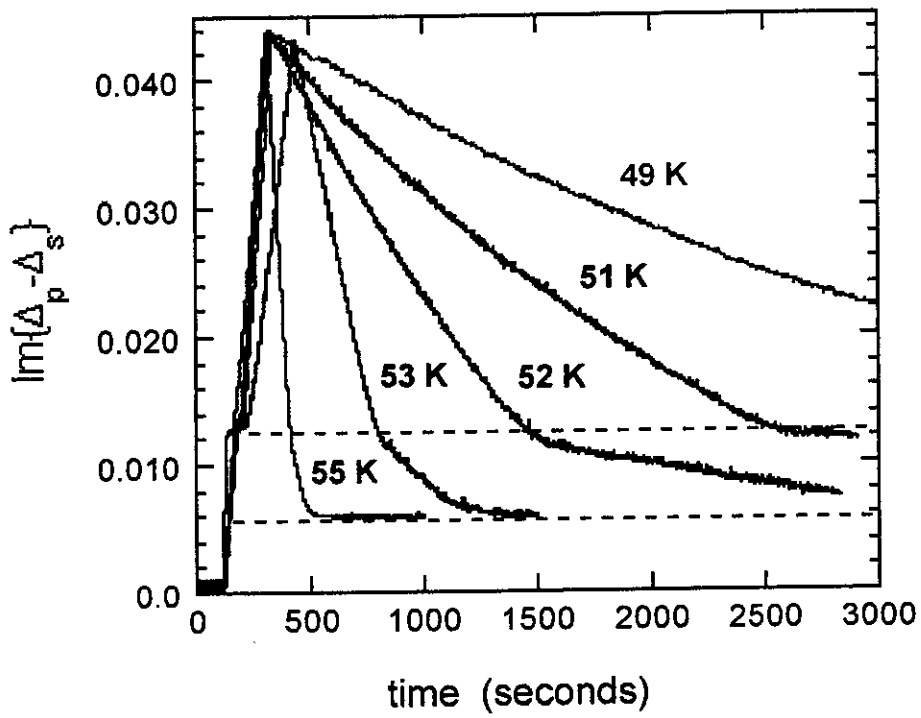

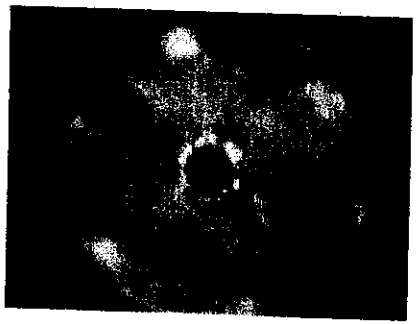

After flashing

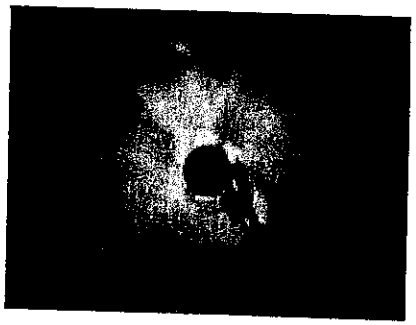

10 L

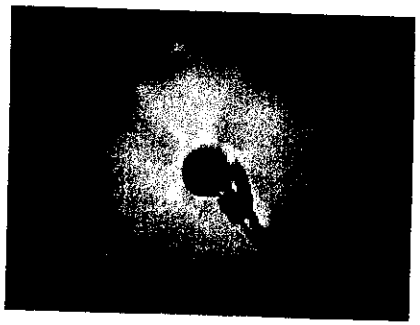

20 L

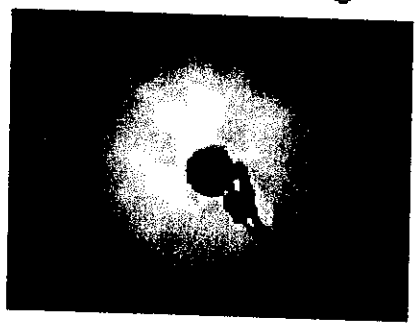

40 L

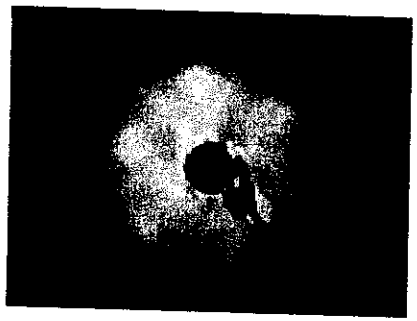

60 L

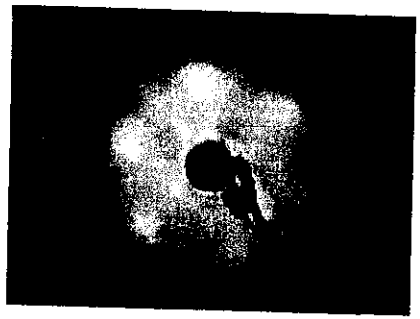

100 L

140 L

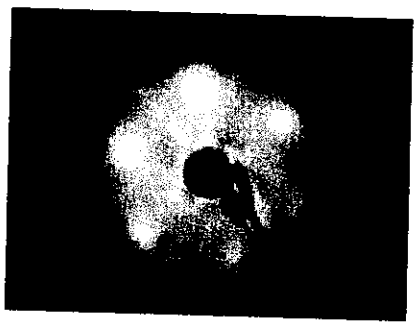

180 L

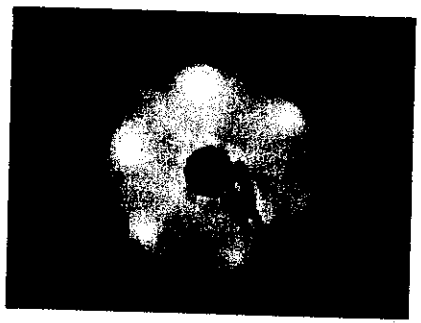

280 L

Step-flow growth of Xe on 2-ML "buffer" Xe on Nb(110)

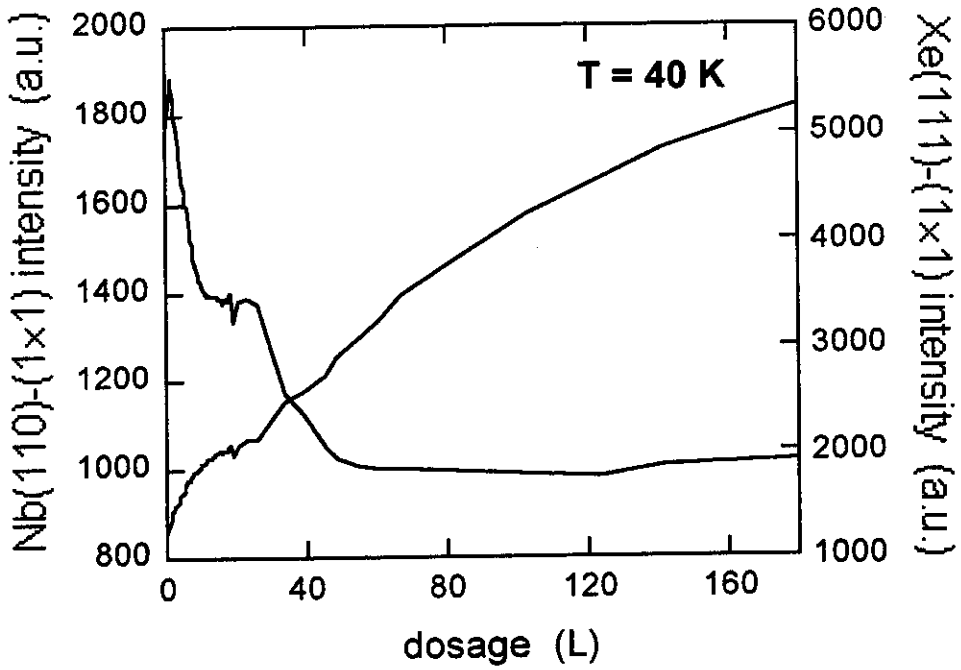

Calculated reflectivity difference for step-flow growth:

$$\varepsilon_d = \varepsilon_{Xe} = 2.0$$

$$\varepsilon_s = \varepsilon_{Nb} = -\ 0.25\ +\ i\,16.13$$

$$\Delta_p - \Delta_s \approx i\left\{\frac{4\pi\cos\phi\sin^2\phi\,\varepsilon_s}{\lambda\left[\varepsilon_s^2\cos^2\phi - \varepsilon_s + \sin^2\phi\right]}\frac{\left(\varepsilon_d - \varepsilon_s\right)\left(\varepsilon_d - 1\right)}{\varepsilon_d}\right\}d$$

$$\approx 5.3\times10^{-3}\left(1 - i\ 0.12\right)\ @\ \mathrm{d} = 3.54\text{Å}$$

Measured reflectivity difference: (40 K ≤ T ≤ 51 K)

$$-\frac{\mathrm{Im}\left\{\Delta_p - \Delta_s\right\}}{\mathrm{Re}\left\{\Delta_p - \Delta_s\right\}} = 0.10 \sim 0.12$$

Adsorption of the 3rd Xe monolayer on 2-ML Xe/Nb(110)

adsorption at edges of stable 2-D clusters

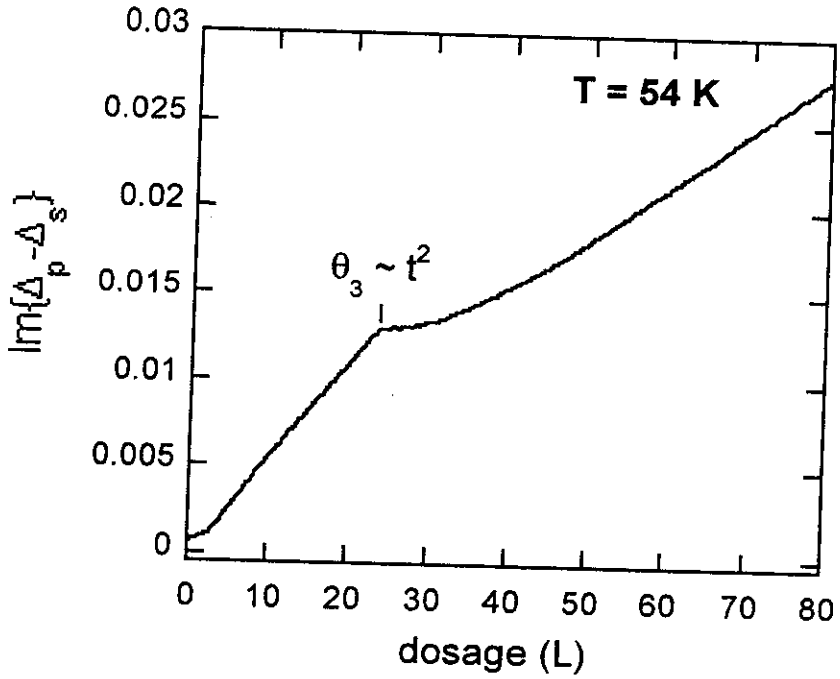

t^2-dependence: $d\theta_3/dt \sim \sqrt{\theta_3}$

- Xe monomers on 2-ML Xe/Nb(110) are short-lived
- Initially, $d\theta_3/dt$ ~ rate of septamer formation
- Adsorption at edges of septamers or larger clusters dominates

$$d\theta_3/dt \sim \sqrt{\theta_3} \qquad \theta_3(t) \sim t^2$$

- Desorption of subsequent Xe layers is rate-limited by detachment from step edges (reversed step-flow)

Zeroth-order desorption and adsorption for overlayers (n ≥ 4)

Competition between step-flow growth and "step-flow" desorption

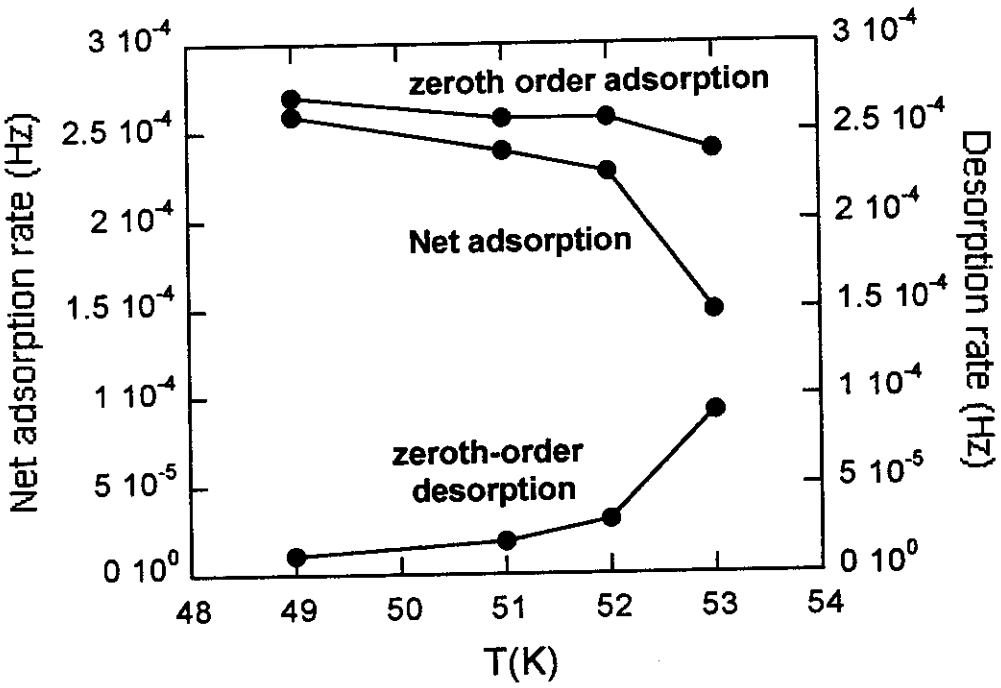

$dN/dt = S(N)\Gamma - N_{s,Xe}\,\nu(T,N)$, N: number of atoms / cm^2

$\nu(T,N)$ independent of N: rate-limited by detachment from step edges (reverse step-flow)

$S(N) \approx S_0 \approx 1$: fast diffusion on Xe(111) terraces toward step edges and efficient capture by step edges

Zeroth-order desorption and adsorption for 2nd Xe overlayer

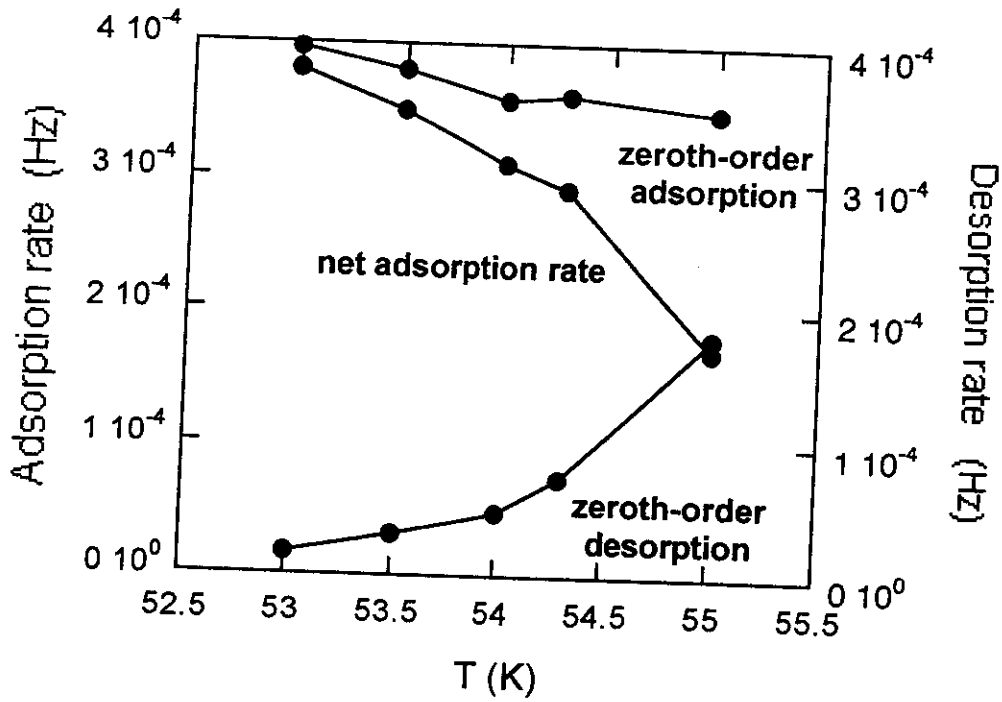

$dN/dt = S(N)\Gamma - N_{s,Xe}\,\nu(T,N)$, N: number of atoms / cm^2

$\nu(T,N)$ weak N-dependence: rate-limited by detachments from island edges or corners, and minorly from terraces directly

$S(N) \approx S_0 \approx 1$: efficient accomodation on terraces of the first Xe ML.

Desorption kinetics of differrent Xe layers on Nb(110)

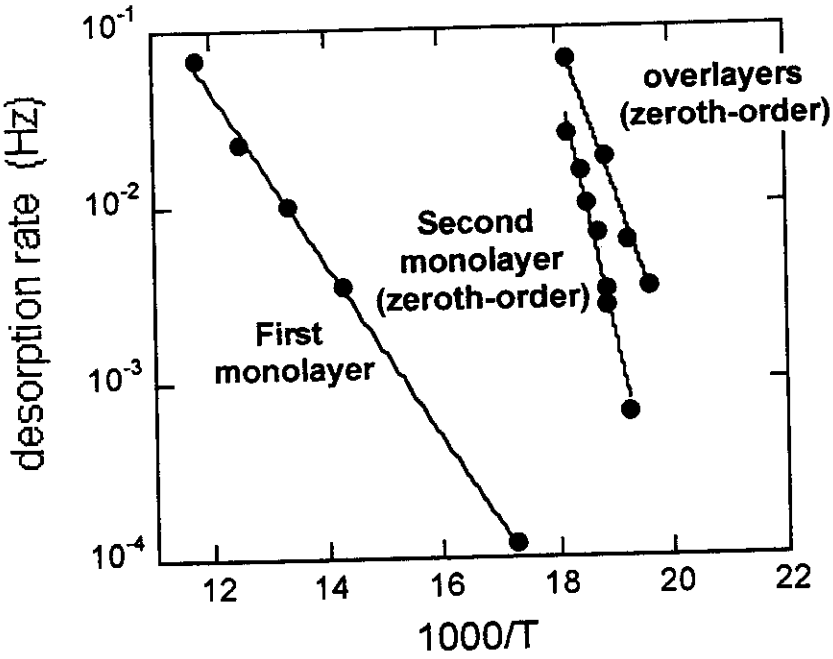

- **First monolayer**

$$\nu_1(T) = 4 \times 10^4 \exp\left(-0.1eV/k_B T\right)$$

- **Second monolayer**

$$\nu_2(T) = 2 \times 10^{26} \exp\left(-0.3eV/k_B T\right)$$

- **Subsequent layers**

$$\nu_{n\geq 3}(T) = 5 \times 10^{15} \exp\left(-0.19eV/k_B T\right)$$

Surface oxidation kinetics in oxide epitaxy

Surface oxidation kinetics in perovskite oxide epitaxy

$SrTiO_3$ on $SrTiO_3$(001)

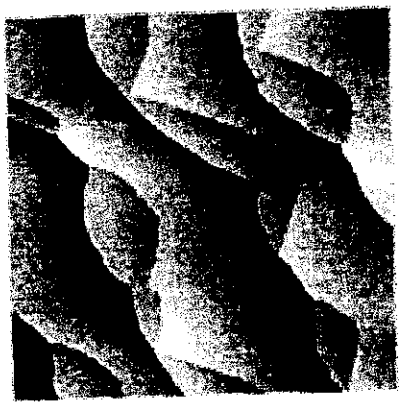

1 μm × 1 μm

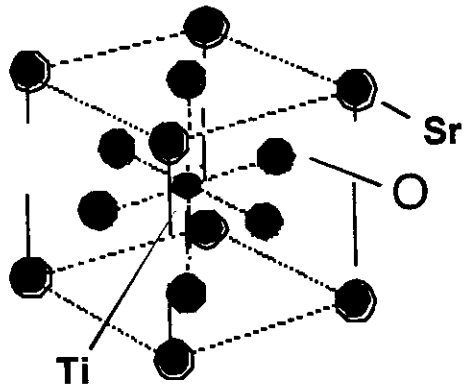

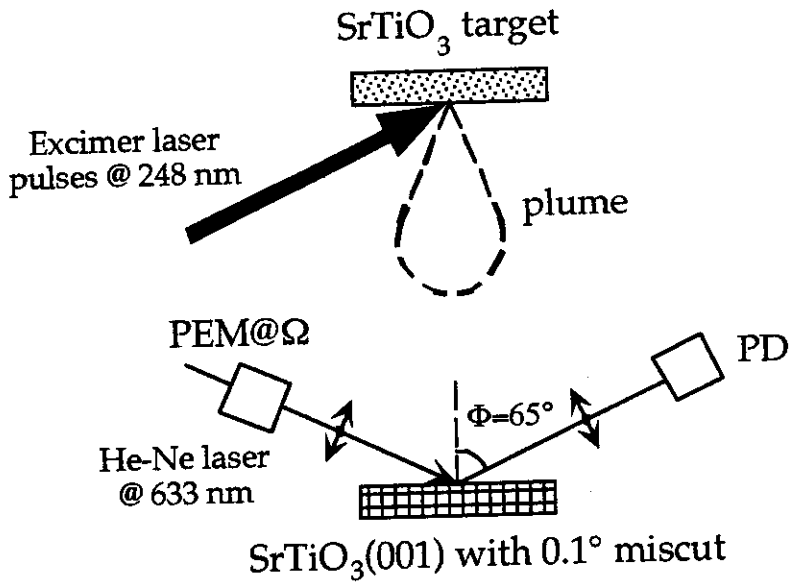

STO Optical constant:	$\varepsilon_s = 5.66 + i\,0$ @ 633 nm
Temperature:	270 ~ 800 °C (550 ~ 1070 K)
Oxygen pressure:	3×10^{-4} ~ 0.6 torr
PLD rate:	0.3 ~ 0.5 ML/sec

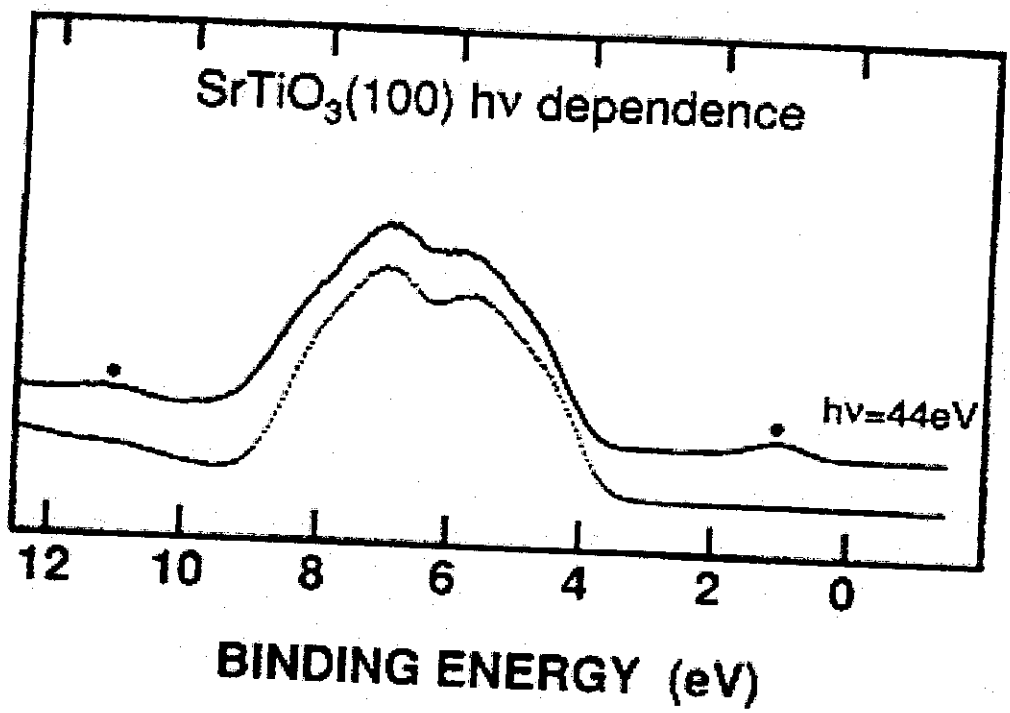

- **Oxygen vacancies in TiO_2 planes induce "defect states" at 1.2 eV below the Fermi surface**

- **Defect states cause optical absorption at λ = 633 nm with $h\nu$ = 1.9 eV**

- $\varepsilon_d \cong \varepsilon_s + \delta\varepsilon_d' + i\,\delta\varepsilon_d''$ **with** $\delta\varepsilon_d''$ **proportional to oxygen vacancy density in the deposited monolayer**

$$\delta\varepsilon_d = \delta\varepsilon_d' + i\,\delta\varepsilon_d'' \approx (-i)\left\{\frac{\lambda\left[\varepsilon_s^2\cos^2\phi - \varepsilon_s + \sin^2\phi\right]}{4\pi d\cos\phi\,\sin^2\phi\left(\varepsilon_s - 1\right)}\right\}\left(\Delta_p - \Delta_s\right)$$

Optical reflectivity difference measurements ($I_{2\Omega}$):

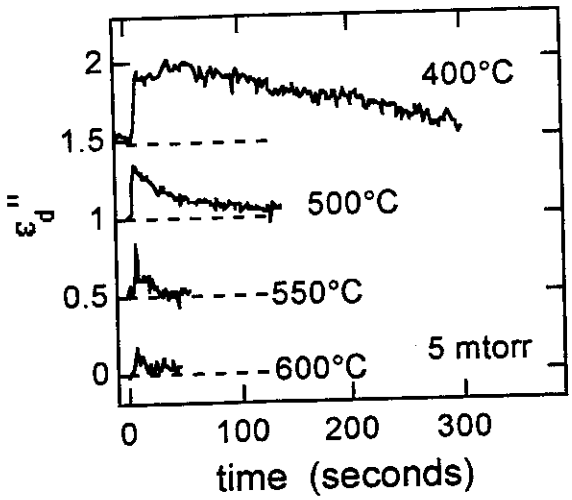

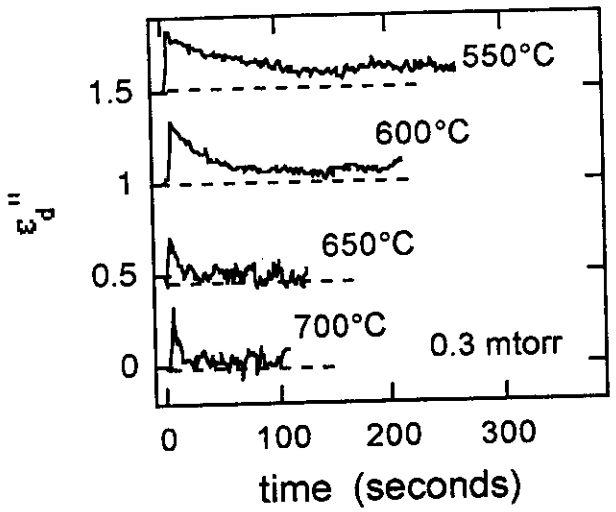

$$\varepsilon_d'' = \delta\varepsilon_d'' \sim \exp\left[-\kappa\left(T, P_{O2}\right)t\right]$$

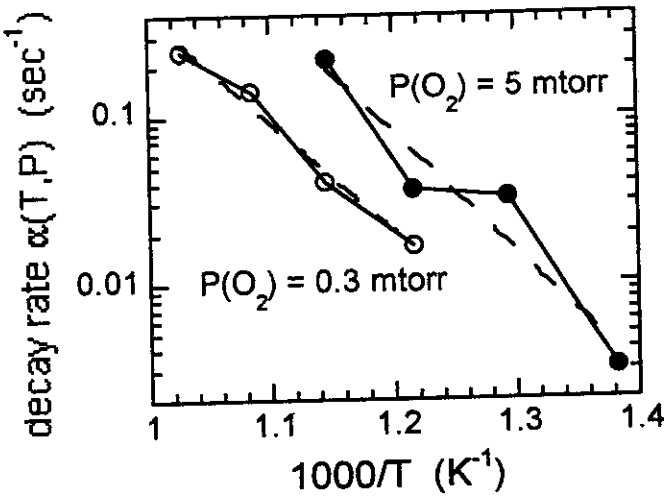

Oxidation reaction parameters:

$$\kappa\left(T, P_{O_2}\right) = \alpha_0 \exp\left(-E_a / k_B T\right) P_{O_2}$$

$E_a = 1.35$ eV

$\alpha_0 = 4 \times 10^9$ torr^{-1} sec^{-1}

Oxidation reaction in the homoepitaxy of $SrTiO_3(001)$

Growth of monolayer oxide in pulsed-laser deposition:

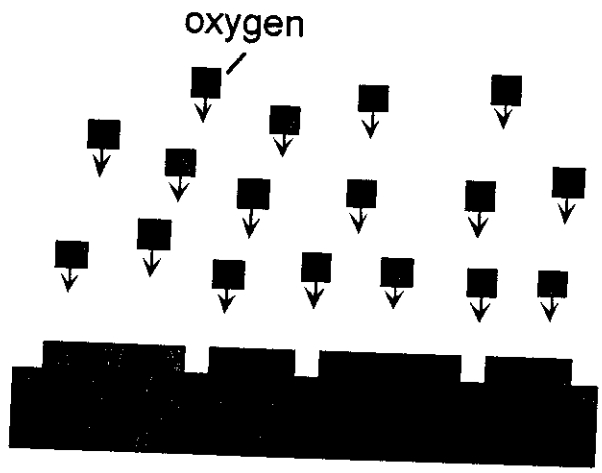

ε_d deviates from ε_s due to incomplete oxidation.

Oxidation reaction during the post-growth treatment:

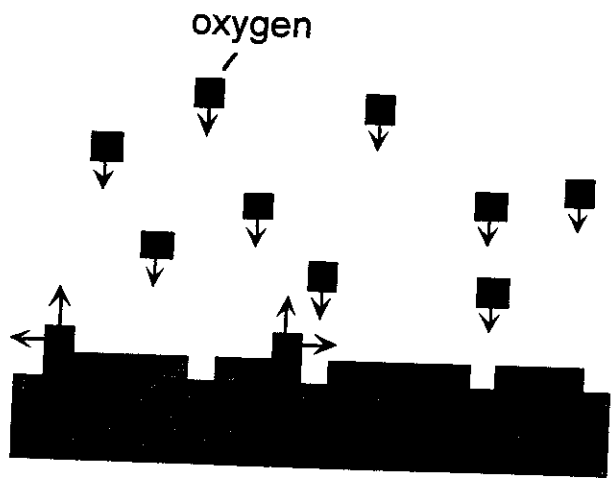

ε_d restores to ε_s as the oxidation reaction is completed.

Oxidation reaction parameters:

$$\kappa\left(T,P_{O_2}\right) = \alpha_0 \exp\left(-E_a/k_B T\right)P_{O_2}$$

$E_a = 1.35$ eV

$\alpha_0 = 4\times 10^9$ torr^{-1} sec^{-1}

(1) Molecular oxygen dissociate near oxygen vacancies (N_v) into oxygen adatoms in a precursor state (N_i);
(T-dependence)

(2) Precursor-state oxygen either desorb (E_{des}) or react with near-by oxygen vacancies (E_R);

$$\frac{dN_i}{dt} = S\Gamma_p\left[\frac{\left(N_{v0}-N_v\right)-N_i}{N_s}\right] - \nu_{des}N_i \exp\left(-E_{des}/k_B T\right) - \nu_R N_i \exp\left(-E_R/k_B T\right)$$

$$\frac{dN_v}{dt} = -\nu_R N_i \exp\left(-E_R/k_B T\right)$$

(3) Desorption rate is large compared to reaction rate such that $N_i \approx \left[S\Gamma_p\left(N_{v0}-N_v\right)/N_s\nu_{des}\right]\exp\left(E_{des}/k_B T\right)$. Consequently,
(P-dependence)

$$N_v \cong N_{v0}\exp\left[-\alpha\left(P_{O_2},T\right)t\right]$$

$$\alpha\left(P_{O_2},T\right) = \left(S\Gamma_p/N_s\right)\left(\nu_R/\nu_{des}\right)\exp\left[-\left(E_R-E_{des}\right)/k_B T\right]$$

Activation energy barrier E_a: $E_a = E_R - E_{des}$

$La_{0.67}Ba_{0.33}MnO_3$ (LBMO) heteroepitaxy on $SrTiO_3(001)$:

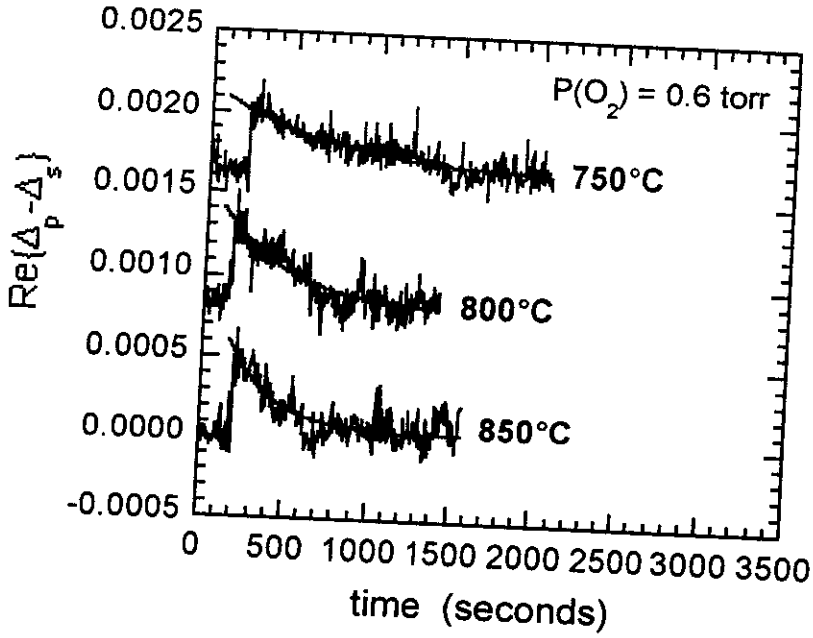

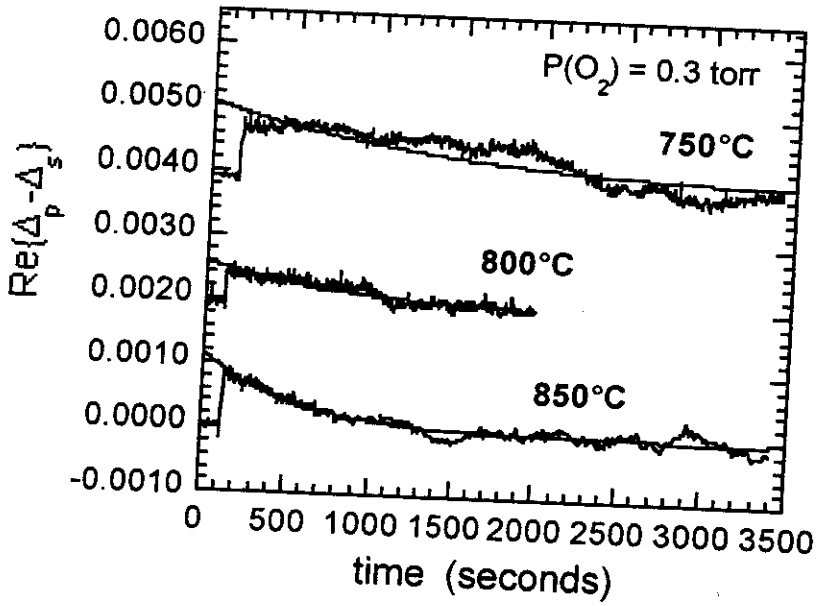

Oxidation reaction parameters: $\kappa\left(T, P_{O_2}\right) = \alpha_0 \exp\left(-E_a/k_B T\right) P_{O_2}$

$E_a = 1.0$ eV

$\alpha_0 = 180$ torr^{-1} sec^{-1}

Thermal annealing of ion-sputtered metal surfaces

Ion sputtering and thermal annealing of a crystalline surface:

ε_d is proportional to the edge atom density

Sputtering:

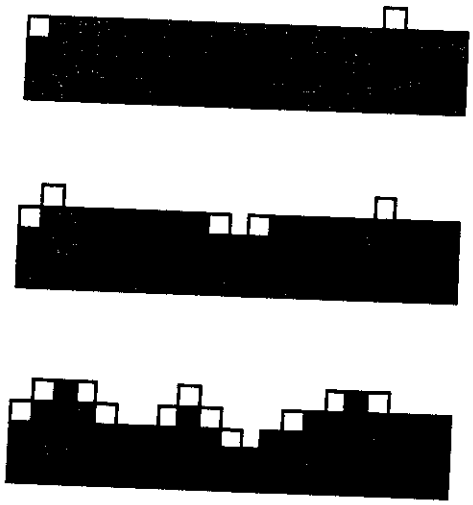

ε_d changes from ε_s monotonically.

Thermal annealing:

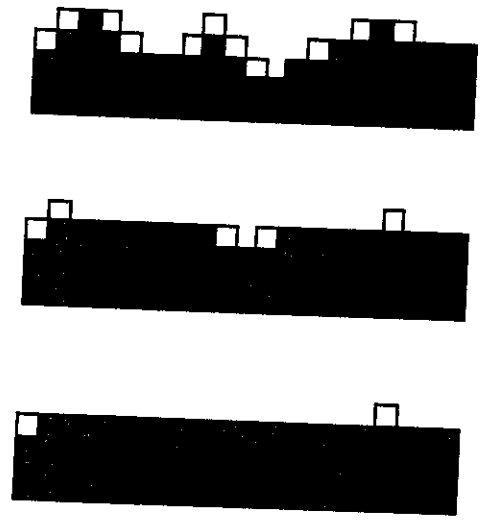

ε_d restores to ε_s monotonically.

Ne^+ ion sputtering and thermal annealing of Ni(111):

Beam energy = 1000 eV, Beam current ~ 2 μA

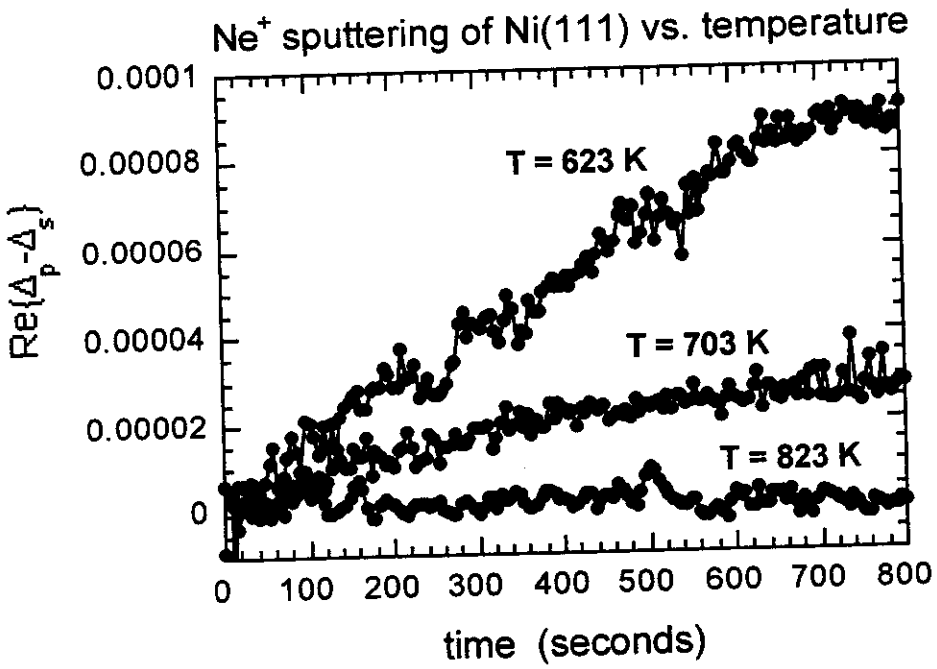

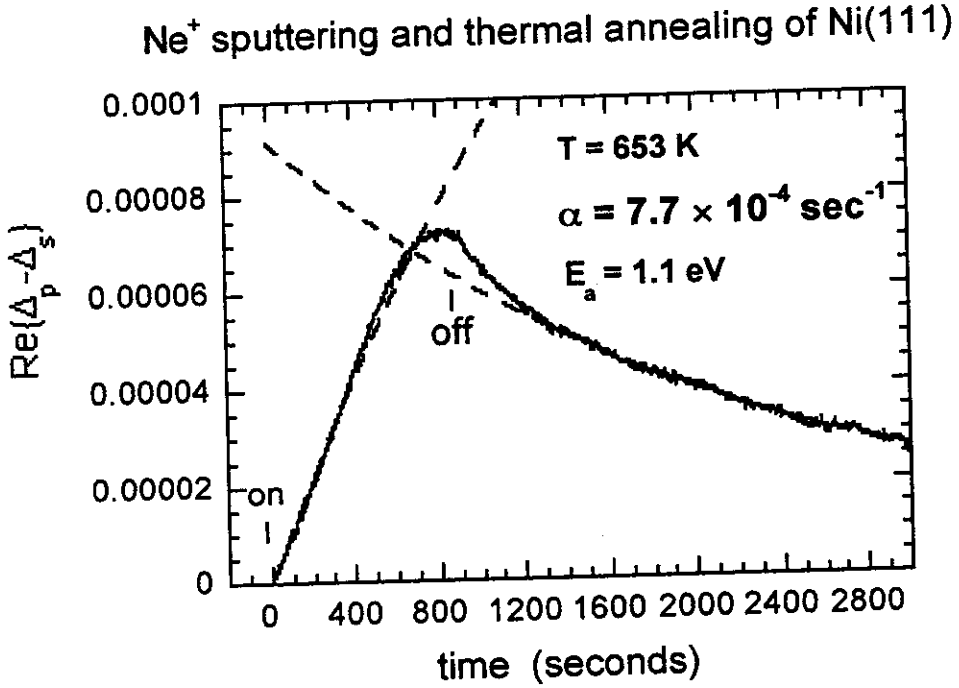

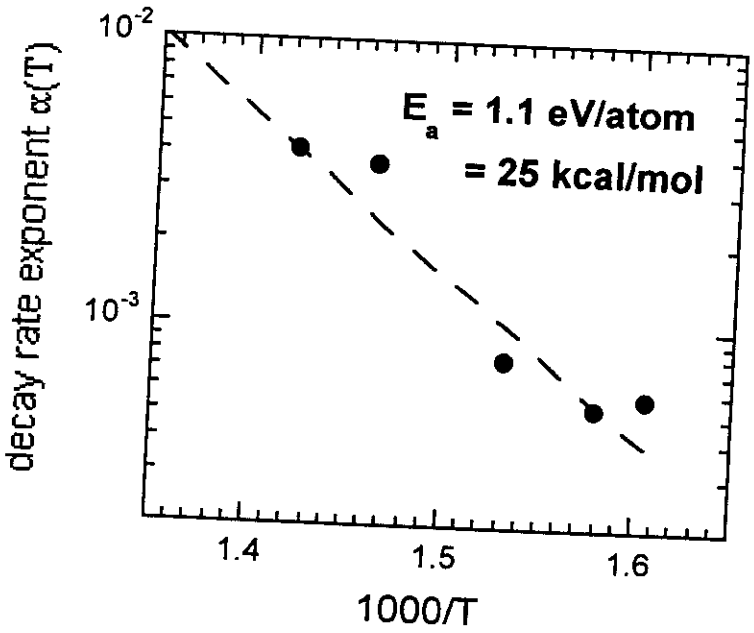

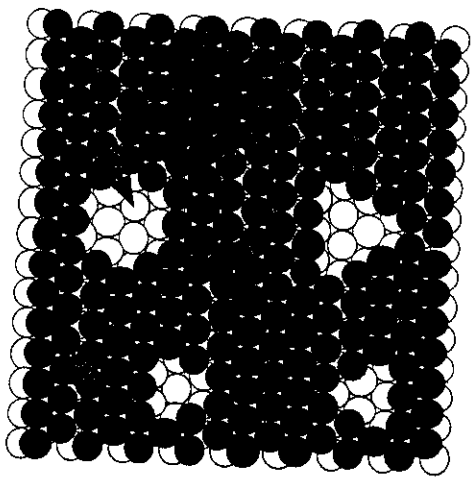

Rate-limiting processes to the thermal annealing of Ni(111):

- Diffusion on Ni(111) terraces: E_{diff}
- **Stepping down B-type edges:** $E_{se} = E_{step} - E_{diff}$
- Evaporation from corners: E_c
- **Evaporation from kinks:** E_{kink}

$E_a \approx E_{kink} + E_{diff} + E_{se}$ (~ 1 eV for Cu on Cu(111))

[Icking-Konert et al., Surf. Sci (1998); Giesen et al., Surf. Sci. (1999); Feibelman, Phys. Rev. Lett. (1998)]

Acknowledgment:

Experiment Edward Nabighian (U.C. Davis/Intel Corp)

Petros Thomas (U.C. Davis)

Weidong Si (Penn State)

Xiaoxing Xi (Penn State)

Qi Li (Penn Sate)

Qidu Jiang (U. of Houston)

M.G. Medici (U. of Houston)

Theory: Maria C. Bartelt (Sandia National Lab)

Finding: NSF-DMR (U.C. Davis, Penn State, U. Houston)

U.S. DoE (Sandia National Lab)

ACS-PRF (U.C. Davis)

T.L. Temple Foundation (U. of Houston)

John and Rebecca Moores Endowment (U. H.)